

# MIR181A regulates starvation- and rapamycin-induced autophagy through targeting of ATG5

Kumsal Ayse Tekirdag,<sup>1,†</sup> Gozde Korkmaz,<sup>1,†</sup> Deniz Gulfem Ozturk,<sup>1</sup> Reuven Agami<sup>2</sup> and Devrim Gozuacik<sup>1,\*</sup>

<sup>1</sup>Faculty of Engineering and Natural Sciences; Biological Sciences and Bioengineering Program; Sabanci University; Istanbul, Turkey; <sup>2</sup>Division of Gene Regulation; The Netherlands Cancer Institute; Amsterdam, The Netherlands

<sup>†</sup>These authors contributed equally to this work.

**Keywords:** macroautophagy, mammalian autophagy regulation, microRNA, hsa-miR-181a, ATG5, starvation, rapamycin, MTOR

**Abbreviations:** ACTB, actin beta; *ATG5*, autophagy-related 5; *ATG12*, autophagy-related 12; *ATG16L1*, autophagy-related 16-like 1; *BECN1*, Beclin 1; miRNA, microRNA; *LC3*, microtubule-associated protein 1 light chain 3; *MIR181A*, human microRNA-181A and its gene; PE, phosphatidylethanolamine; MTOR, mechanistic target of rapamycin; MRE, miRNA-response element; *BCL2*, B-cell lymphoma 2; *RPS6KB/P70S6K*, ribosomal protein S6 kinase; *SQSTM1/P62*, sequestosome 1; *RAP*, rapamycin; *STV*, starvation; *E+P*, E64d/pepstatin A; *RT-PCR*, reverse transcriptase-polymerase chain reaction; *MTT*, thiazolyl blue tetrazolium blue; *Ant-181a*, *MIR181A*-specific antagomir; *CNT-Ant*, control antagomir; *TRIZOL*, trizol Reagent; *PEI*, polyethylenimine; *DMSO*, dimethyl sulfoxide; *U6*, U6 small nuclear 1 (RNU6-1); *GFP*, green fluorescent protein; *MIR376B*, human microRNA-376B and its gene; *EBSS*, Earle's Balanced Salt Solution; *MIR30A*, human microRNA-30A and its gene; *QPCR*, quantitative PCR; *GAPDH*, glyceraldehyde-3-phosphate dehydrogenase

Macroautophagy (autophagy herein) is a cellular catabolic mechanism activated in response to stress conditions including starvation, hypoxia and misfolded protein accumulation. Abnormalities in autophagy were associated with pathologies including cancer and neurodegenerative diseases. Hence, elucidation of the signaling pathways controlling autophagy is of utmost importance. Recently we and others described microRNAs (miRNAs) as novel and potent modulators of the autophagic activity. Here, we describe *MIR181A* (hsa-miR-181a-1) as a new autophagy-regulating miRNA. We showed that overexpression of *MIR181A* resulted in the attenuation of starvation- and rapamycin-induced autophagy in MCF-7, Huh-7 and K562 cells. Moreover, antagomir-mediated inactivation of endogenous miRNA activity stimulated autophagy. We identified *ATG5* as an *MIR181A* target. Indeed, *ATG5* cellular levels were decreased in cells upon *MIR181A* overexpression and increased following the introduction of antagomirs. More importantly, overexpression of *ATG5* from a miRNA-insensitive cDNA construct rescued autophagic activity in the presence of *MIR181A*. We also showed that the *ATG5* 3' UTR contained functional *MIR181A* responsive sequences sensitive to point mutations. Therefore, *MIR181A* is a novel and important regulator of autophagy and *ATG5* is a rate-limiting miRNA target in this effect.

## Introduction

Autophagy is a highly conserved catabolic pathway of the cell, degrading long-lived proteins and damaged organelles.<sup>1</sup> Autophagy is active at a basal level under normal conditions, but is rapidly upregulated following exposure to stress factors including nutrient/hormone deprivation, hypoxic stress, accumulation of misfolded proteins or bacterial invasion.<sup>2,3</sup> Autophagy plays important roles in various organismal processes such as development and aging and abnormalities in autophagy lead to pathologies including neurodegenerative diseases and cancer.<sup>4-7</sup>

The hallmark of autophagy is the formation of double- or multimembrane vesicles in the cytosol called autophagosomes. These vesicles eventually fuse with lysosomes to form autolysosomes where cargo degradation occurs using lytic enzymes.<sup>1,8</sup>

There are several important protein complexes acting in concert during autophagosome formation including the *ATG12*–*ATG5*–*ATG16L1* and *ATG8* (or *MAP1LC3*, abbreviated in the text as *LC3*, in mammals) conjugation systems.<sup>9</sup> In the first system, following a ubiquitination-like reaction involving E1- and E2-like enzymes *ATG7* and *ATG10*, respectively, the *ATG12* ubiquitin-like protein is covalently conjugated to the intermolecular lysine 130 of the *ATG5* protein. Then, *ATG12*–*ATG5* forms a larger complex with, and oligomerizes through, *ATG16L1*.<sup>9</sup> In the second ubiquitination-like reaction, *LC3* protein is covalently conjugated to the lipid PE (phosphatidylethanolamine) and this event is necessary for autophagic membrane elongation and vesicle completion.<sup>10</sup> In addition to the activity of *ATG7* (E1-like) and *ATG3* (E2-like) enzymes, *LC3*-lipid conjugation requires the E3-like activity of *ATG12*–*ATG5*–*ATG16L1* complex.<sup>11</sup> To

\*Correspondence to: Devrim Gozuacik; Email: dgozuacik@sabanciuniv.edu  
Submitted: 04/19/12; Revised: 12/03/12; Accepted: 12/04/12  
<http://dx.doi.org/10.4161/auto.23117>

be primed for conjugation, a C-terminal glycine residue of LC3 has to be exposed following its cleavage by ATG4 proteins.<sup>12,13</sup>

While free LC3 (also called LC3-I) is soluble, its lipid-conjugated form (LC3-II) is associated with growing and complete autophagosomes. Hence, LC3 conjugation is used as a molecular marker of autophagosome generation and accumulation.<sup>12</sup> A second autophagy marker is degradation of the autophagy receptor SQSTM1/p62, reflecting autolysosomal lytic activity and autophagic flux.<sup>14</sup>

Mechanisms regulating mammalian autophagy still need further investigation. Accumulating data indicate that, in addition to intracellular signaling mechanisms, miRNAs play an important and central role in autophagy regulation.<sup>15,16</sup> miRNAs are ~22 nucleotide-long noncoding RNAs that are expressed endogenously in various organisms from plants to mammals.<sup>17</sup> They control biological events by either triggering degradation of their target mRNAs, and/or through inhibition of their translation. They do so selectively, by recognizing specific sequences called miRNA-response elements (MREs), generally present in the 3' UTR of target mRNAs.<sup>18</sup>

Recent reports provided evidence that under stress conditions, a number of miRNAs including *MIR30A*, *MIR101*, *MIR130A*, and *MIR196* are capable of modulating autophagic activity by changing intracellular levels of key autophagy proteins.<sup>19–22</sup> Indeed, as a result of an unbiased miRNA screen, we discovered that *MIR376B* regulated autophagy by directly targeting autophagy genes *BECN1* (Beclin 1 gene) and *ATG4C*.<sup>23</sup> Another miRNA that we discovered during this screen was *MIR181A1*/hsa-miR-181a-1/hsa-miR-213 (abbreviated as *MIR181A* herein). Here, we describe the role of this miRNA in the control of autophagy. We demonstrated that *MIR181A* blocked starvation- and rapamycin-induced autophagy in cancer cell lines. In light of our results, we provide evidence for a key autophagy protein, ATG5, as a rate-limiting and direct autophagy-related target of *MIR181A*.

## Results

***MIR181A* blocked starvation-induced autophagy in MCF-7 cells.** An unbiased screen using GFP-LC3 as a read-out and starvation as a stimulus in MCF-7 cells that we described recently,<sup>23</sup> led us to identify *MIR181A* (miRbase accession number: MI0000289) as a novel microRNA potentially regulating autophagy. The *MIR181* family consists of at least four members, namely *MIR181A-D*, and they were shown to play important roles in various biological events including development, differentiation, hematopoiesis, immune modulation and muscle adaptation to exercise.<sup>24</sup> *MIR181A* is widely expressed in several tissues including brain, thymus, and bone marrow and its levels were shown to change in response to stress.<sup>25–27</sup>

We first confirmed that *MIR181A* had an effect on autophagy. As shown in **Figure 1A and B**, overexpression of *MIR181A* significantly blocked starvation-induced GFP-LC3 dot accumulation. In line with these results, starvation-activated lipid conjugation of free LC3-I to the autophagic membrane-associated LC3-II was attenuated in the extracts of cells following *MIR181A*

transfection (**Fig. 1C**) and degradation of the autophagy receptor SQSTM1 following starvation was less in miRNA-transfected cell extracts (**Fig. 1D**). These results introduced *MIR181A* as a new miRNA controlling autophagy.

It should be noted that LC3-I migrated as a double band in some immunoblots. Since two unrelated antibodies recognized both bands, in this paper we considered both bands as LC3-I (**Fig. S1** and see *Materials and Methods* for details).

***MIR181A* blocked rapamycin-induced autophagy in MCF-7 cells.** We then checked whether *MIR181A* overexpression also had an effect on rapamycin-induced autophagy. Rapamycin stimulates autophagy through inhibition of MTOR (mammalian target of rapamycin).<sup>28</sup> In line with starvation-related results, rapamycin-induced GFP-LC3 dot formation (**Fig. 1E and F**), LC3 lipidation (**Fig. 1G**) and SQSTM1 degradation (**Fig. 1H**) were decreased following overexpression of *MIR181A*. Therefore, we concluded that, in addition to its effects on starvation-induced autophagy, *MIR181A* also inhibited rapamycin-induced autophagic activity in MCF-7 cells.

**Effect of *MIR181A* on autophagy was observed in two more cell lines.** In order to check whether the miRNA effects that we observed in the MCF-7 breast cancer cell line were cell type-specific or not, we performed autophagy tests in two other cell types, Huh-7 cells (a human hepatocarcinoma cell line) and K562 cells (a human chronic myelocytic leukemia cell line). *MIR181A* overexpression in Huh-7 cells significantly attenuated starvation- and rapamycin-induced GFP-LC3 dot formation (**Fig. 2A and B; Fig. 2E and F**, respectively). Similar to the results in MCF-7 cells, overexpression of *MIR181A* resulted in a decrease in stimulus-activated LC3-I/LC3-II conversion (**Fig. 2C and G**) and SQSTM1 degradation (**Fig. 2D and H**) in Huh-7 cells. In line with these data, both LC3-I/LC3-II conversion and SQSTM1 degradation were attenuated in K562 cells overexpressing *MIR181A* but not the control miRNA (**Fig. S2**).

These results showed that *MIR181A* blocked autophagy in at least three cell lines originating from different tissues. Therefore, the effect of *MIR181A* on autophagy might be cell-type independent.

**Tests with lysosomal protease inhibitors.** To confirm that *MIR181A* inhibited autophagy-induced LC3 turnover and SQSTM1 degradation, and therefore autophagic vesicle flux, we performed similar autophagy tests in the presence or absence of lysosomal protease inhibitors E64d and pepstatin A. Indeed, addition of the lysosomal inhibitors led to a prominent accumulation of LC3-II and SQSTM1 in *MIR-CNT* transfected cells, pointing to the presence of a normal autophagic flux under these conditions. Yet, since *MIR181A* blocked autophagic vesicle generation, inhibitor-related accumulation of LC3-II and SQSTM1 during starvation was relatively less in MCF-7 cells overexpressing *MIR181A* compared with controls (**Fig. S3A and S3B**). Similar results were obtained in Huh-7 cells following autophagy stimulation by starvation (**Fig. S3E and S3F**). Rapamycin stimulus also led to similar results in both cell types (**Fig. S3C and S3D; Fig. S3G and S3H**).

To further confirm these results, we also followed the appearance of free GFP in GFP-LC3 transfected cells in the presence

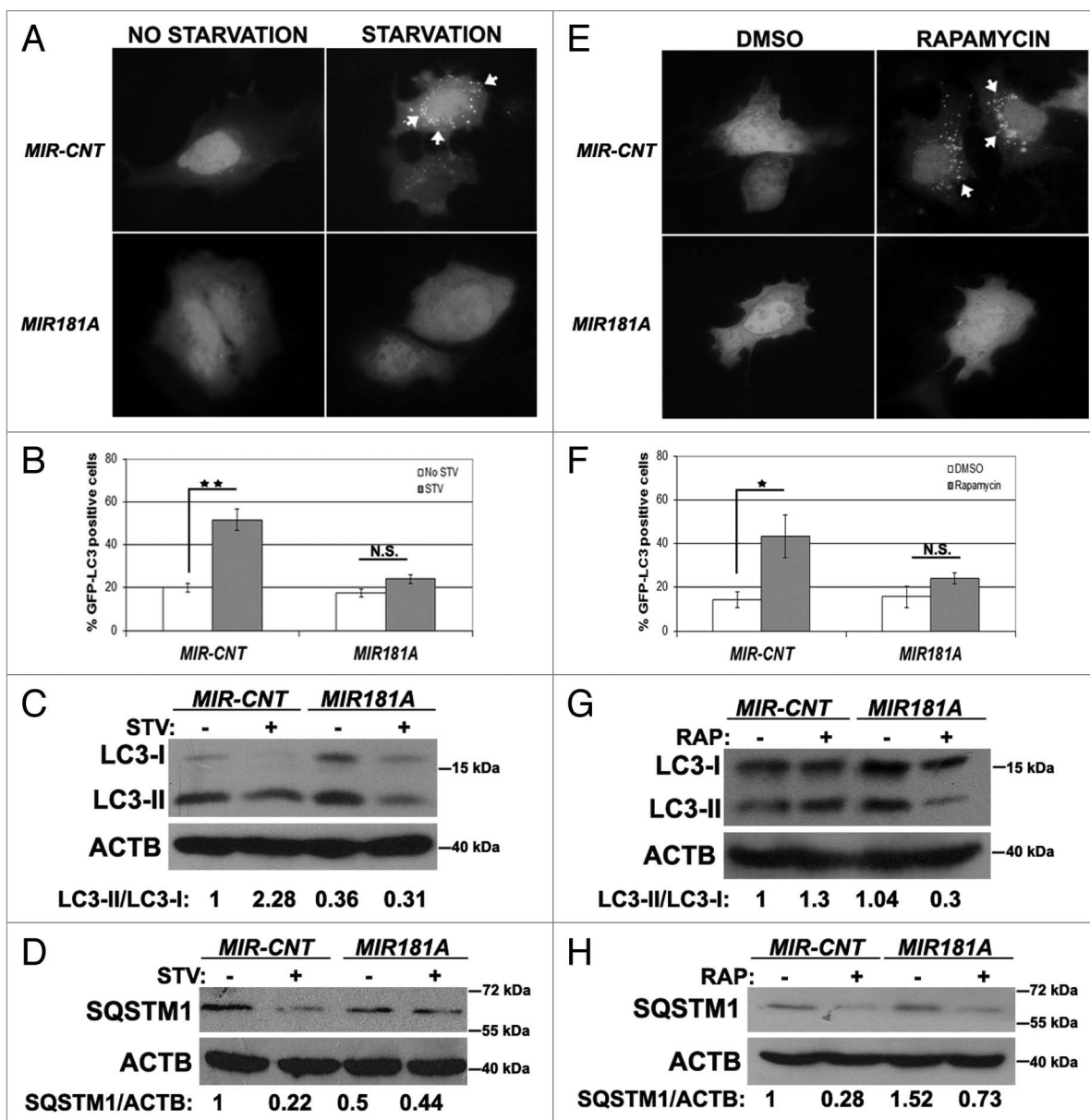


**Figure 1.** Overexpression of *MIR181A* resulted in decreased autophagic activity in MCF-7 cells. (A) *MIR181A* blocked starvation-induced GFP-LC3 dot formation in MCF-7 cells. Cells were cotransfected with *MIR181A* or control construct (*MIR-CNT*) together with GFP-LC3 plasmid and autophagy was assessed under no starvation or starvation (2 h) conditions. White arrows indicate clusters of the GFP-LC3 dots in cells. (B) Quantitative analysis of the experiments in (A). *MIR181A* overexpression, but not control (*MIR-CNT*) overexpression, blocked starvation-induced autophagy (mean  $\pm$  SD of independent experiments,  $n = 3$ , \*\* $p < 0.01$ . N.S., not significant). (C) *MIR181A* decreased starvation-induced conversion of LC3-I to LC3-II in MCF-7 cells. Immunoblot results of extracts from nonstarved (STV-) or starved (STV+) cells ( $n = 3$ ). LC3-II/LC3-I densitometric ratios are marked. ACTB was used as a loading control. (D) *MIR181A* blocked starvation induced SQSTM1 degradation in MCF-7 cells ( $n = 3$ ). ACTB was used as a loading control. SQSTM1/ACTB densitometric ratios were marked. (E) *MIR181A* blocked rapamycin-induced GFP-LC3 dot formation. Cells were cotransfected with GFP-LC3 plasmid and *MIR181A* or *MIR-CNT*, treated with DMSO (carrier) or rapamycin (2.5  $\mu$ M, 24 h). (F) Quantitative analysis of the experiments in (E) (mean  $\pm$  SD of independent experiments,  $n = 4$ , \* $p < 0.05$ . N.S., not significant). (G) *MIR181A* decreased LC3-I to LC3-II conversion stimulated by rapamycin (RAP) in MCF-7 cells ( $n = 2$ ). LC3-II/LC3-I ratios are marked. (H) *MIR181A* blocked rapamycin-induced SQSTM1 degradation in MCF-7 cells ( $n = 2$ ).

or absence of lysosomal hydrolase inhibitors. It was previously reported that free GFP fragments generated from the lysosomal cleavage of GFP-LC3 accumulated best during rapamycin treatment, and under these conditions for stimulating autophagy, addition of late-stage autophagy inhibitors such as E64d/pepstatin A further increased free GFP levels.<sup>29,30</sup> As shown in Figure

S4, following rapamycin treatment, a free GFP band appeared on the blots. Addition of E64d/pepstatin A resulted in a further increase in free GFP band intensity in controls but not in *MIR181A*-overexpressing cells. Hence, attenuation of autophagic activity by *MIR181A* led to a lower amount of GFP-LC3 degradation and free GFP accumulation in cell expressing the miRNA.

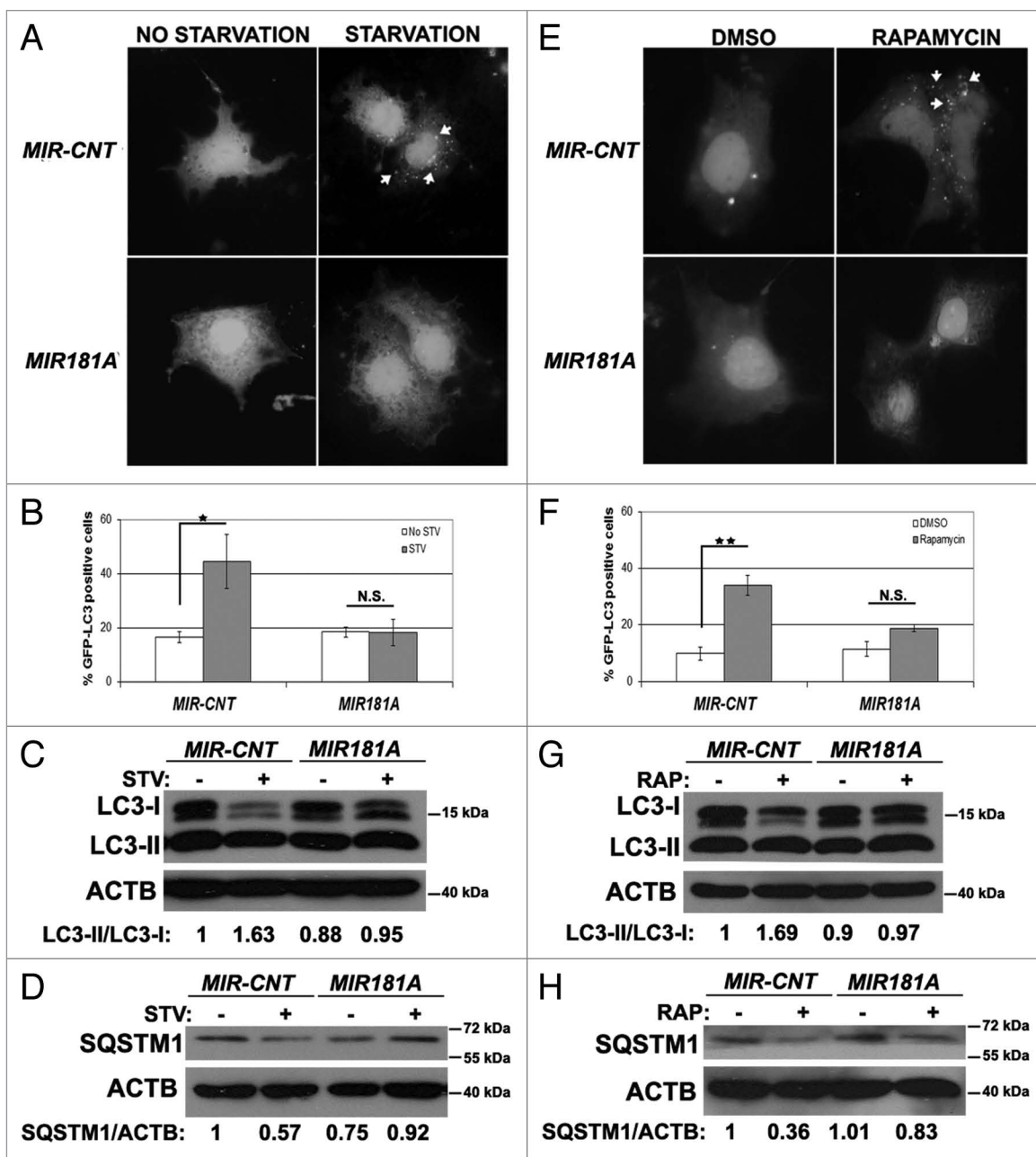


**Figure 2.** Effect of *MIR181A* on autophagy is not cell-type dependent. (A) *MIR181A* blocked starvation-induced GFP-LC3 dot formation in Huh-7 cells. Cells were cotransfected with GFP-LC3 plasmid and *MIR181A* or *MIR-CNT* and autophagy was assessed under no starvation or starvation (4 h) conditions. (B) Quantitative analysis of the experiments in (A) (mean  $\pm$  SD of independent experiments,  $n = 3$ , \* $p < 0.05$ . N.S., not significant). (C) *MIR181A* expression decreased starvation-induced LC3-I to LC3-II conversion in Huh-7 cells ( $n = 3$ ). LC3-II/LC3-I ratios are marked. (D) *MIR181A* blocked starvation-induced SQSTM1 degradation in Huh-7 cells ( $n = 2$ ). SQSTM1/ACTB ratios are marked. (E) *MIR181A* blocked rapamycin-induced GFP-LC3 dot formation. Autophagy was assessed following DMSO or rapamycin treatment (2.5  $\mu$ M, 24 h). (F) Quantitative analysis of the experiments in (E) (mean  $\pm$  SD of independent experiments,  $n = 3$ , \*\* $p < 0.01$ . N.S., not significant). (G) *MIR181A* resulted in decreased rapamycin-induced conversion of LC3-I to LC3-II in Huh-7 cells ( $n = 2$ ). RAP, rapamycin. LC3-II/LC3-I ratios are marked. (H) *MIR181A* blocked rapamycin-induced SQSTM1 degradation in Huh-7 cells ( $n = 2$ ). SQSTM1/ACTB ratios are marked.

Effect of antagomir-mediated inhibition of endogenous *MIR181A* on autophagy. Antagomirs, or anti-miRNAs, counteract miRNA effects by specifically inhibiting endogenous mature miRNAs. To test the effects of endogenous *MIR181A* inhibition on autophagy, we transfected cells with *MIR181A*-specific antagomirs (Ant-181a) or control antagomirs (CNT-Ant) and

analyzed autophagy under nonstarved or starved conditions. We observed that starvation-dependent GFP-LC3 dot formation was modestly but significantly increased (Fig. 3A and B) and LC3-I to LC3-II conversion was stimulated (Fig. 3C), hence autophagy was accelerated in cells transfected with Ant-181a but not with control antagomirs. Moreover, SQSTM1 degradation following

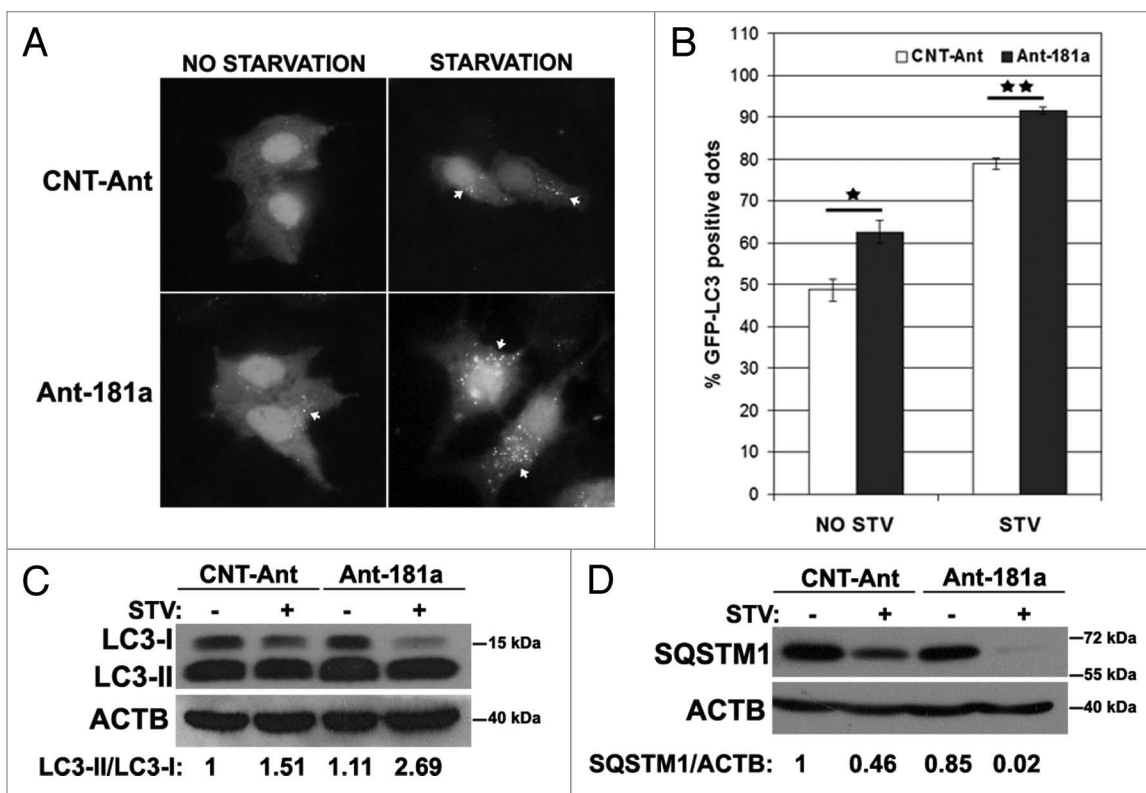


**Figure 3.** Inhibition of endogenous *MIR181A* using antagonomirs (Ant-181a) stimulated autophagic activity. (A) Ant-181a enhanced starvation-induced GFP-LC3 dot formation. CNT-Ant, control antagonomirs. (B) Quantitative analysis of the experiments in (A). NO STV, No starvation. STV, starvation for 20 min. (mean  $\pm$  SD of independent experiments,  $n = 3$ , \* $p < 0.05$ , \*\* $p < 0.01$ ). (C) Ant-181a, but not CNT-Ant stimulated starvation (STV, 4 h)-stimulated LC3-I to LC3-II conversion in MCF-7 cells ( $n = 4$ ). LC3-II/LC3-I densitometric ratios are marked. (D) Ant-181a, but not CNT-Ant resulted in the stimulation of SQSTM1 protein degradation following starvation (4 h) in MCF-7 cells ( $n = 3$ ). SQSTM1/ACTB ratios are marked.

starvation was more prominent after Ant-181a transfection compared with controls (Fig. 3D). Therefore, inhibition of endogenous *MIR181A* using antagonomirs led to a further stimulation of the autophagic activity during starvation, indicating that endogenous *MIR181A* contributes to the limitation of stress-activated autophagic responses in cells.

**Autophagy-related target of *MIR181A*.** To unravel the mechanism of autophagy inhibition by *MIR181A*, we searched for autophagy genes containing potential *MIR181A* MREs in their 3' UTRs using publicly available bioinformatics tools Microcosm Targets and TargetScan. *ATG5* (GenBank accession number: NM\_004849.2, 1177–1200) was identified as a *MIR181A* target by both bioinformatics tools. The predicted interaction between *MIR181A* and the *ATG5* 3' UTR was shown in Figure 4A. To confirm the bioinformatics-based predictions, we performed immunoblot analysis in control or *MIR181A* transfected cell extracts using an *ATG5*-specific antibody. Indeed, *ATG5* protein levels were decreased in MCF-7 cells that were overexpressing *MIR181A* under both fed and starved conditions (Fig. 4B). Similarly, *ATG5* protein levels were decreased in *MIR181A* transfected Huh-7 (Fig. S5A) and K562 cells (Fig. S5B). miRNA expression also affected target transcript levels in cells. A decrease in *ATG5* mRNA levels was observed by qPCR in cells following transfection with *MIR181A* but not with *MIR-CNT* (Fig. 4C). Conversely, introduction of the antagonomir Ant-181a (blocking

endogenous *MIR181A*), but not control antagonomirs, resulted in an increase in *ATG5* protein levels in cells (Fig. 4D).

To further validate that *ATG5* downregulation was responsible for the autophagy-related effects of *MIR181A*, we performed “rescue experiments.” In these experiments, *ATG5* protein was overexpressed from a plasmid lacking the *MIR181A* response element; it was therefore resistant to miRNA-mediated downregulation. Hence, although *MIR181A* overexpression decreased endogenous *ATG5* protein levels significantly, cells cotransfected with the miRNA and the *ATG5* plasmid possessed near physiological (approx. 1.36x) levels of total *ATG5* protein (Fig. 5A). Under these conditions, the *MIR181A*-mediated suppression of autophagy observed during starvation-induced autophagy was reversed upon co-expression of the *ATG5* protein (Fig. 5B and C). In other words, introduction of the *ATG5* protein was sufficient to bring autophagy back to normal levels even in the presence of the miRNA. These results demonstrated that *ATG5* was the rate-limiting target of *MIR181A* for autophagy inhibition.

**Other potential autophagy-related targets.** BCL2, an anti-apoptotic member of the BCL2 family that was involved in autophagy regulation through sequestration of the autophagy protein BECN1, is among the known targets of *MIR181A*.<sup>31–34</sup> In our system, overexpression of the miRNA did not significantly affect the levels of BCL2 protein under nonstarved or starved conditions in MCF-7 cells (Fig. S6A), whereas, in line with other

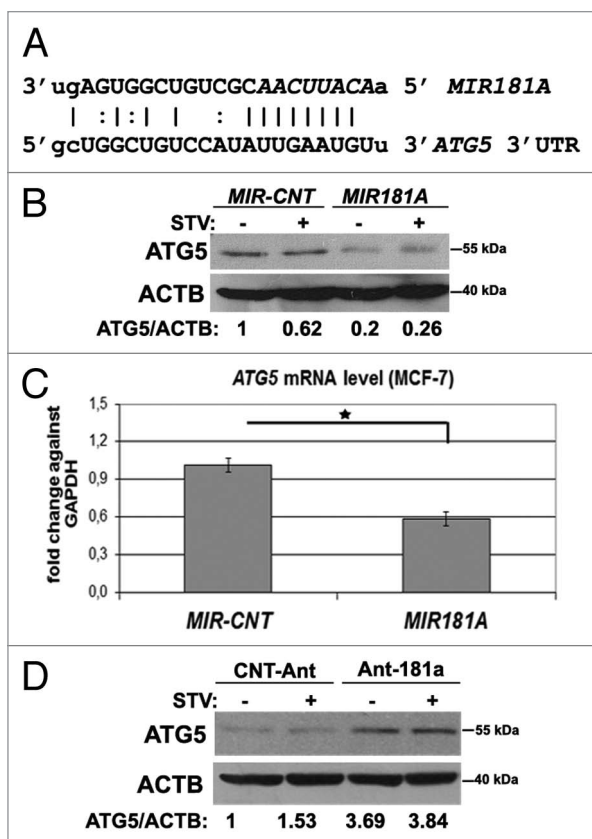


**Figure 4.** *MIR181A* affected ATG5 levels in MCF-7 cells. (A) *MIR181A* target sequence in the 3' UTR of the *ATG5* mRNA. The *MIR181A* seed sequence is marked in italics. (B) ATG5 protein levels were decreased following *MIR181A* overexpression in MCF-7 cells. Immunoblots of *MIR-CNT* or *MIR181A* transfected cells that were nonstarved (STV-) or starved (STV+) (n = 3). ACTB was used as a loading control. ATG5/ACTB band densitometric ratios are shown. (C) Quantitative PCR (qPCR) analysis of *ATG5* mRNA levels in control (*MIR-CNT*) or *MIR181A* transfected MCF-7 cells (mean  $\pm$  SD of independent experiments, n = 3, \*p < 0.05). Data were normalized using *GAPDH* mRNA. (D) ATG5 protein levels were increased following antagomir-181a (Ant-181a) transfection. CNT-Ant, control antagomirs (n = 2). ATG5/ACTB ratios are shown.

reports,<sup>35,36</sup> there was no detectable BCL2 protein expression in Huh-7 cells (Fig. S6B). Therefore, we think that BCL2 regulation by *MIR181A* did not contribute to the autophagy modulatory effects described here.

We also checked whether there are other autophagy-related targets of *MIR181A*. Since *MIR181A* could block MTOR inhibitor rapamycin-induced autophagy, and ATG5 is downstream of MTOR in the autophagy pathway, we wondered whether the upstream MTOR pathway would be affected by the overexpression of this miRNA. To check the effect of *MIR181A* on MTOR activity, we analyzed the phosphorylation status of an MTOR target protein, RPS6KB/p70S6K. Although under basal/fed condition overexpression of *MIR181A* led to an unexpected increase in RPS6KB phosphorylation, this difference between *MIR181A* and control transfected cells vanished following autophagy activation by starvation (Fig. S7). Thus, although it is possible that *MIR181A*-induced MTOR-activation could contribute to its

autophagy-blocking effects, miRNA overexpression could not overcome starvation-induced MTOR inhibition in our hands.

We also checked the effect of *MIR181A* overexpression on previously identified autophagy-related miRNA targets.<sup>23</sup> We found that *MIR181A* overexpression had no significant effect on the levels of the *MIR30A* and *376B* target BECN1 protein, or the *MIR376B* target ATG4C protein (Fig. S8A and S8B).

Using the bioinformatics tools mentioned above, we next analyzed *ATG5* and *ATG12* mRNA 3' UTRs for *MIR376B*-specific MREs. The *ATG12* 3' UTR but not that of *ATG5* contained a potential *MIR376B* response element (Fig. S8C). In qPCR tests, we observed no change in *ATG12* transcript levels in *MIR376B* overexpressing cells (Fig. S8D). On the other hand, *MIR376B* overexpression could result in a decrease in ATG12-ATG5 protein complex levels (Fig. S8E). Therefore, *MIR376B* might potentiate the inhibitory effect of *MIR181A* on autophagy, possibly through regulation of ATG12 protein levels. Further studies are needed to resolve this issue.

All together we concluded that, although it is possible that some other targets of *MIR181A* could contribute to its biological effects, ATG5 seems to be the major and rate-limiting autophagy-related target of this microRNA.

**ATG5 as direct target of *MIR181A*.** To further validate the effect of *MIR181A* on ATG5, the region in the 3' UTR of the *ATG5* mRNA containing a potential *MIR181A* response element was cloned into the 3' UTR part of a luciferase vector. In parallel, we also created a mutant version of this construct by introducing base changes to the crucial binding residues, mainly in the miRNA seed sequence-binding region (Fig. 6A). Cotransfection of *MIR181A* together with the wild-type luciferase vector in 293T cells resulted in a significant decrease in the luciferase activity compared with control levels (Fig. 6B, wild-type). In contrast, *MIR181A* had no significant effect on the levels of luciferase expressed from the mutant construct; here the luciferase activity was similar to control levels (Fig. 6B, mutant). These results showed that, *MIR181A* controlled the levels of ATG5 by directly targeting the above described MRE present in the 3' UTR region of the *ATG5* gene.

**Effect of autophagy inducers on endogenous *MIR181A* levels.** We wondered whether *MIR181A* endogenous miRNA levels were responsive to the stress-inducing stimuli used in this study. We starved cells for 2 or 4 h, or treated them with the MTOR-inhibitor rapamycin. Interestingly, starvation did not lead to a significant change in the miRNA levels (Fig. 6C). In contrast, rapamycin treatment induced a prominent increase in endogenous *MIR181A* levels (Fig. 6D). Since *MIR181A*-specific antagomir introduction could further lead to an increase in the target ATG5 protein levels (see above), we believe that even under starvation conditions, steady-state endogenous levels of the miRNA were still functional to counteract autophagy. Yet, we showed that *MIR181A* levels might be upregulated in response to certain stress-stimuli such as rapamycin.

## Discussion

In this study, we introduced *MIR181A* as a novel autophagy-related microRNA. *MIR181A* overexpression inhibited GFP-LC3

dot formation, LC3-I to LC3-II conversion and SQSTM1 degradation. These results were valid for two commonly used autophagy stimuli, namely starvation and rapamycin and in at least three cell types originating from different tissues (MCF-7 breast cancer, Huh-7 liver cancer and K562 chronic myelocytic leukemia cell lines). Additionally, antagomir-mediated suppression of cellular endogenous *MIR181A* was shown to accelerate the autophagic response. All together, these data established that *MIR181A* is one of the key miRNAs in autophagy regulation.

We identified *ATG5* as a target of *MIR181A*. We showed that *MIR181A* overexpression attenuated *ATG5* protein and mRNA levels and, more importantly, reintroduction of *ATG5* protein in the presence of *MIR181A* reversed autophagy blockage by the miRNA. The effect of *MIR181A* on *ATG5* was direct since the MRE found in the 3' UTR region of the *ATG5* gene was responsive to *MIR181A*, and introduction of mutations to this sequence abolished the miRNA effect. So, our results established *ATG5* as a rate-limiting and important target of *MIR181A* during autophagy regulation.

Results presented in this work may be summarized in a model as follows (Fig. 7). Cellular *ATG5* amount above a certain threshold is required to form functional *ATG12-ATG5-ATG16L1* complexes, subsequent LC3 lipidation and autophagy activation. The presence of miRNAs including *MIR181A* under stress conditions leads to a fall in *ATG5* levels below the threshold, and therefore results in a decrease in LC3 lipidation and inhibition of autophagic activity. So, stress signals stimulating autophagy seem to be counteracted by inhibitor miRNAs such as *MIR181A*, limiting uncontrolled and potentially harmful autophagic activity in cells.

While this manuscript was in preparation, Huang et al. published a report suggesting a connection between *ATG5* and *MIR181A*.<sup>37</sup> Working on the mechanisms of cisplatin resistance in squamous cell carcinoma cells JHU-029, they discovered that a TP63 isoform  $\alpha$ ,  $\Delta Np63\alpha$ , downregulated *MIR181A*.<sup>37,38</sup> In this context, they showed that *MIR181A* inhibitors led to an increase in *ATG5* protein levels and, mimics and inhibitors of the miRNA modulated expression from a luciferase construct fused to the full length 3' UTR region of *ATG5*.<sup>37</sup> Yet, the importance of *MIR181A* or *ATG5* downregulation for cisplatin-induced autophagy is still obscure, and the above-mentioned study did not experimentally refine a *MIR181A* response element in *ATG5* mRNA. Nevertheless, possible involvement of *MIR181A* in the regulation of autophagy activated by stimuli other than starvation or rapamycin is intriguing.

Another autophagy-related miRNA, *MIR30A*, was recently shown to regulate *ATG5* levels in chronic myeloid leukemia (CML) cells including K562.<sup>39</sup> In this report, *MIR30A* overexpression decreased and antagomirs against this miRNA increased *BECN1* and *ATG5* levels. Interestingly, *MIR30A*-mediated changes in *BECN1* and *ATG5* levels and modulation of cytoprotective autophagy influenced the efficacy of the BCR-ABL tyrosine kinase inhibitor drug imatinib on CML cells. Likewise, *MIR181A* was able to affect *ATG5* levels and autophagy in K562

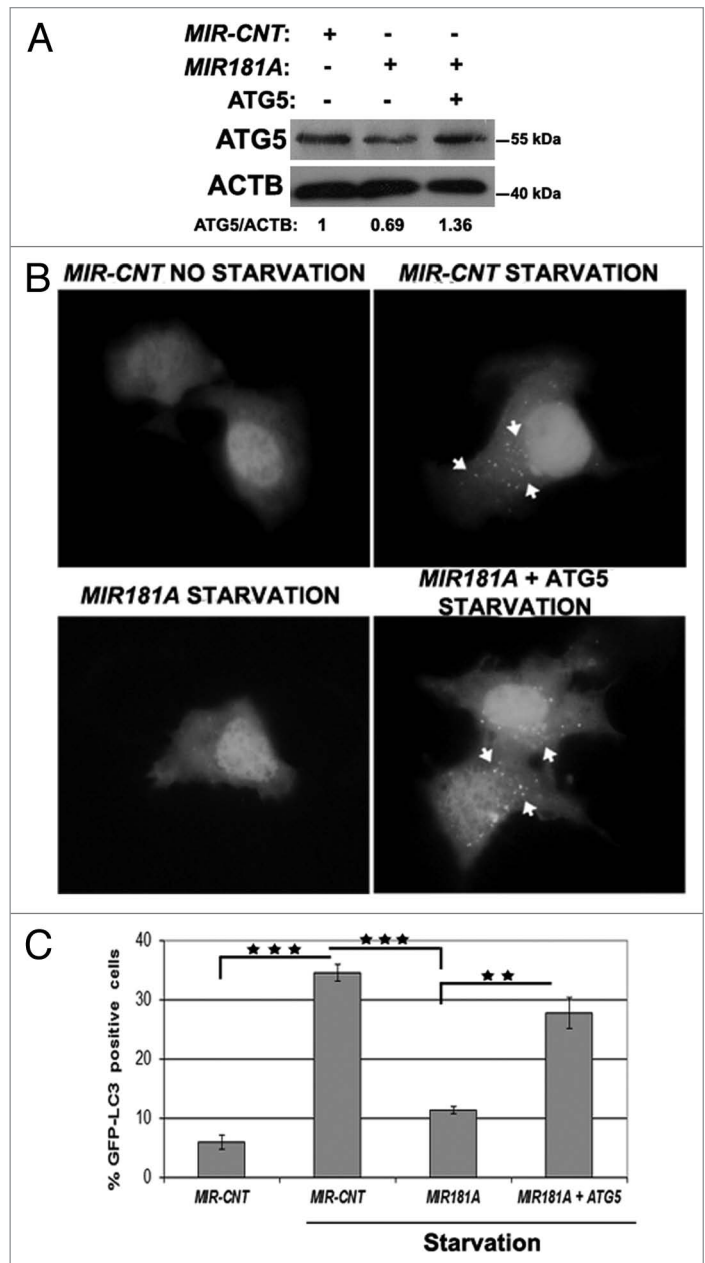


**Figure 5.** *ATG5* overexpression rescued cells from *MIR181A*-mediated autophagy inhibition. MCF-7 cells were cotransfected with *MIR181A* or *MIR-CNT* and an *ATG5* expression plasmid lacking the *MIR181A* target region. Autophagy was evaluated. (A) Immunoblot analysis of showing *ATG5* and *ACTB* protein levels following indicated transfections ( $n = 2$ ). *ATG5/ACTB* ratios are shown. (B) GFP-LC3 dot formation before or after starvation (2 h). *ATG5*, *MIR181A*-insensitive *ATG5* expression plasmid. (C) Quantitative analysis of GFP-LC3 dot formation (mean  $\pm$  SD of independent experiments,  $n = 3$ , \*\* $p < 0.01$  and \*\*\* $p < 0.001$ ).

CML cells. Yet, the influence of *MIR181A* on imatinib responses and its possible crosstalk with *MIR30A* needs to be studied. Of note, *MIR30A* overexpression did not influence endogenous *MIR181A* levels in cells (Fig. S9).

*MIR181A* was previously shown to be involved in various events including development, differentiation, hematopoiesis,

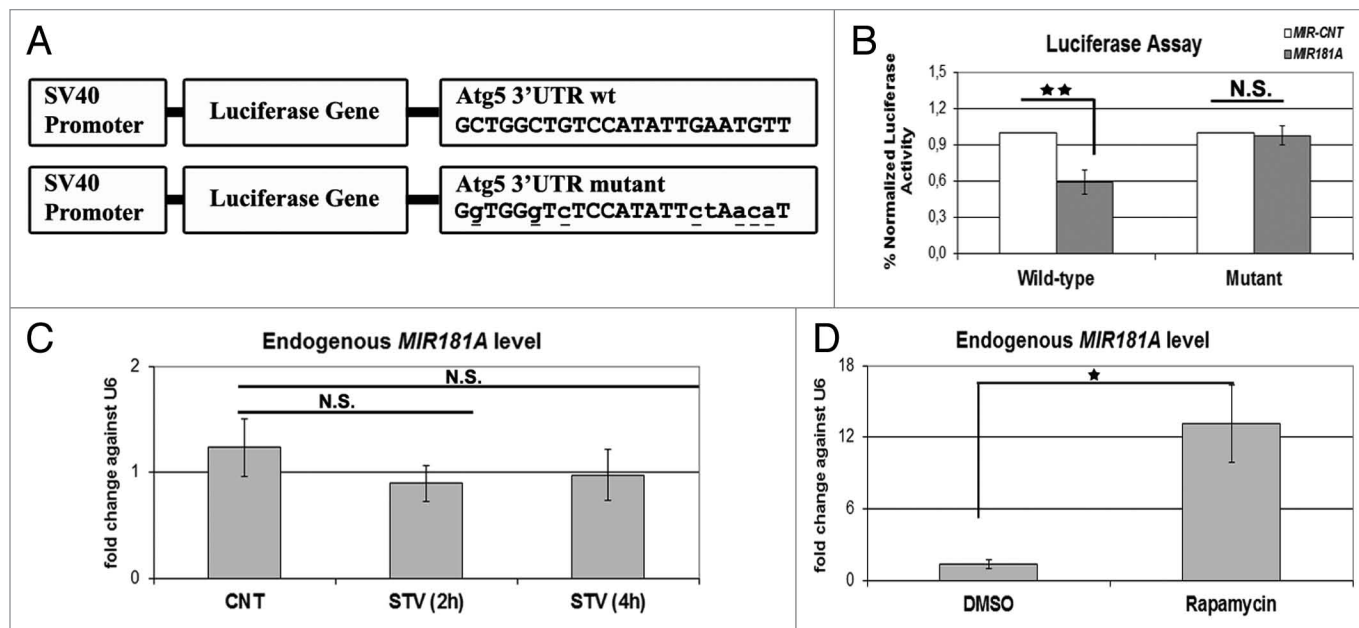


**Figure 6.** ATG5 as a direct target of *MIR181A* and changes in endogenous *MIR181A* levels during cellular stress. **(A)** A scheme representing luciferase constructs with wild-type (wt) or mutant 3' UTR *MIR181A* MRE sequences of *ATG5*. Mutations are marked in lower case letters and underlined. **(B)** Normalized luciferase activity in lysates from 293T cells co-transfected with wild-type or mutant *ATG5*-luciferase constructs and *MIR181A* or *MIR-CNT* (mean  $\pm$  SD of independent experiments,  $n = 3$ , \*\* $p < 0.01$ . N.S., not significant). **(C)** TaqMan quantitative PCR (qPCR) analysis of endogenous *MIR181A* levels under control (CNT, no starvation) or starvation (STV, 2 h and 4 h) conditions. Endogenous *MIR181A* levels were not responsive to starvation treatment (mean  $\pm$  SD of independent experiments,  $n = 3$ , N.S., not significant). TaqMan qPCR data were normalized using *U6 small nuclear 1 (RNU6-1)* (*U6*) mRNA levels. **(D)** TaqMan qPCR analysis of endogenous *MIR181A* levels in cells treated with DMSO (carrier) or rapamycin. Endogenous *MIR181A* levels were increased following rapamycin treatment (mean  $\pm$  SD of independent experiments,  $n = 4$ , \* $p < 0.05$ ).

immune modulation and muscle adaptation to exercise.<sup>27,40-42,43,44</sup> In fact, autophagy was described as an important regulator of similar physiological events.<sup>45-47</sup> Study of the contribution of autophagy-related effects of *MIR181A* in these and other overlapping scenarios could provide valuable information about the importance of this miRNA under physiological conditions.

A complex connection exists between autophagy and cancer. Autophagy deficiency was associated with increased tumor formation in animal models and, mutations or epigenetic changes in autophagy genes and proteins were documented in some human cancer types.<sup>48-50</sup> Therefore, autophagy was proposed as a mechanism protecting cells from cancerous transformation.<sup>3,51</sup> On the other hand, some tumor types become addicted to autophagy and under these conditions autophagy seems to control tumor necrosis and inflammation in response to metabolic stress.<sup>52</sup> Hence, autophagy seems to serve as a cancer cell survival mechanism in established tumors. Consequently, the combination of autophagy inhibition with cancer therapy was proposed as a novel approach to potentiate tumor cell death.<sup>7,53</sup> Interestingly, *MIR181A* is downregulated in human squamous cell and non-small-cell lung cancers and, upregulation of the same miRNA is observed in multiple myeloma and head and neck cancers.<sup>54-57</sup> In cancers with a high *MIR181A* expression, autophagy inhibition through *MIR181A*-mediated targeting of *ATG5* might modulate survival responses and contribute to cancer cell sensitization to chemotherapy. In line with this, *MIR181A* overexpression could potentiate the effects of radiation therapy or chemotherapy

agents Ara-C, vincristine and cisplatin in glioma, leukemia, gastric cancer or lung cancer cell lines.<sup>33,34,58,59</sup> Similarly, we could observe that *MIR181A* overexpression potentiated the toxicity of the cancer therapy agent cisplatin in MCF-7 breast cancer cells (Fig. S10). So, at least in cancer types harboring *MIR181A* level changes, autophagy modulation by this miRNA might have an impact on the survival of the transformed cells and affect their responses to chemotherapy. Further studies are required to explore the contribution of *MIR181A* expression to chemotherapy sensitivity of different types of cancers.

## Materials and Methods

**Plasmid constructs.** Details of the microRNA screening procedure and miRNA vectors were previously described.<sup>23,60</sup> As a control, human telomerase RNA (hTR) was used. For the dual luciferase assay, the MRE found in the 3' UTR region of the *ATG5* mRNA and its mutated version were cloned into the pGL3-control vector (Promega E1741) at the 3' region of the luciferase gene using following linker primers: *ATG5* wildtype primers: 5'-CTA GAG CTG GCT GTC CAT ATT GAA TGT TGA ATT CT-3', 5'-CTA GAG AAT TCA ACA TTC AAT ATG GAC AGC CAG CT-3'. *ATG5* mutant primers: 5'-CTA GAG GTG GGT CTC CAT ATT CTA ACA TGA ATT CT-3', 5'-CTA GAG AAT TCA TGT TAG AAT ATG GAG ACC CAC CT-3'. *Xba*I restriction sites between the stop codon and polyadenylation signal were used.



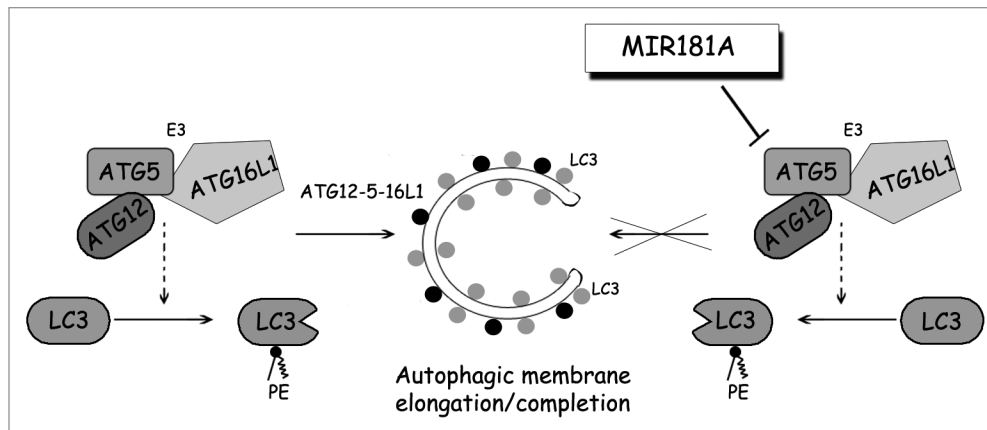


**Figure 7.** A model depicting the effect of *MIR181A* on autophagy pathways. *MIR181A* regulates stress-induced autophagy by targeting the key autophagy protein ATG5. The resulting decrease in ATG12–ATG5–ATG16L1 activity leads to attenuation of LC3 lipidation and inhibits the membrane elongation and completion stage of autophagy.

**Cell culture and transfections.** MCF-7 human breast carcinoma cells, Huh-7 human hepatocellular carcinoma cells and 293T human embryonic kidney cells were cultured in DMEM (Sigma, 05671) supplemented with 10% (v/v) fetal bovine serum (FBS; Biochrom KG, S0115) and antibiotics (Penicillin/Streptomycin; Biological Industries, 03-031-1B) in a 5% CO<sub>2</sub>-humidified incubator at 37°C. K562 cells were cultured in RPMI medium (Invitrogen, 31870) supplemented with 10% FBS and antibiotics. In order to induce autophagy, starvation in Earle's Balanced Salt solution (EBSS; Biological Industries, BI02-010-1A) or rapamycin (2.5 μM, 24 h) (Sigma-Aldrich, R0395) were used.

Transient transfection of MCF-7, Huh-7 and K562 cells was performed using either polyethylenimine (PEI; Polysciences Inc., 23966) transfection method as previously described<sup>23</sup> or AMAXA nucleofector (Lonza Nucleofector II AAD-1001S) with program E-014 and the Nucleofector kit V (Lonza, VCA-1003) according to the manufacturer's instructions. 293T cells were transfected using calcium phosphate coprecipitation method according to standard protocols.<sup>61</sup>

**GFP-LC3 analyses.** Forty-eight hours after cotransfection of miRNAs and GFP-LC3, MCF-7 cells and Huh-7 cells were incubated for 2 h or 4 h in EBSS medium or in DMEM medium/FBS containing 2.5 μM rapamycin for 24 h. Cells were fixed in 3.7% formaldehyde for 20 min, washed with PBS, mounted and inspected under 60× magnification using a BX60 fluorescence microscope (Olympus, BX60). Basal autophagy threshold was determined as 10 GFP-LC3 dots per MCF-7 cell and 15 GFP-LC3 dots per Huh-7 cell. At least 150 GFP positive cells per condition were counted and the graphs were plotted as percentage of GFP-LC3 dot positive cells over total number of transfected cells.

GFP-LC3 analyses of antagomir-transfected cells were done as described above but to better observe differences in the exponential phase of autophagic vesicle formation, tests were performed in the presence of lysosomal protease inhibitors E64d (10 μg/ml) (Santa Cruz, SC201280A) and pepstatin A (10 μg/ml) (Sigma, P5318) and after 20 min of starvation.

**Target prediction for miRNA.** miRNA targets were identified using publicly available bioinformatics tools Microcosm

Targets ([www.ebi.ac.uk/enright-srv/microcosm/htdocs/targets/v5/](http://www.ebi.ac.uk/enright-srv/microcosm/htdocs/targets/v5/)) and TargetScan Human ([www.targetscan.org/](http://www.targetscan.org/)).

**Immunoblot analysis and antibodies.** Protein extraction was performed with RIPA buffer (50 mM TRIS-HCl pH 7.4, 150 mM NaCl, 1% NP40, 0.25% Na-deoxycholate) supplemented with complete protease inhibitor cocktail (Roche, 04-693-131-001) and 1mM phenylmethylsulfonyl fluoride (PMSF; Sigma-Aldrich, P7626). Cell extracts (30 μg) were separated in 15% SDS-polyacrylamide gels and transferred to PVDF membranes (Roche, 03010040001). Following blockage in 5% nonfat milk in PBST (3.2 mM Na<sub>2</sub>HPO<sub>4</sub>, 0.5 mM KH<sub>2</sub>PO<sub>4</sub>, 1.3 mM KCl, 135 mM NaCl and 0.05% Tween 20, pH 7.4) for 1 h at RT, membranes were incubated in 3% BSA-PBST solutions containing primary antibodies (ab): anti-ATG5 ab (Sigma-Aldrich, A0856, dilution 1:2000), anti-LC3B ab (Sigma-Aldrich, L7543, dilution 1:2000), anti-SQSTM1/p62 ab (BD Transduct. Lab, 610832, 1:1000), anti-ACTB ab (Sigma-Aldrich, A5441, dilution 1:7500) and anti-BCL2 ab (Santa Cruz, sc-7382, 1:1000), anti-RPS6KB/p70S6 kinase ab (Cell Signaling, 9202, 1:1000), anti-Phospho-RPS6KB/p70S6 kinase Thr389 ab (Cell Signaling, 9206, 1:1000), anti-GFP ab (Roche, 11-814-460-001, 1:1000). Then, secondary mouse or rabbit antibodies coupled to horseradish peroxidase (anti-mouse: Jackson ImmunoResearch Laboratories, 115035003; anti-rabbit: Jackson ImmunoResearch laboratories, 111035144, dilutions 1:10,000) were applied in 5% milk/PBST for 1 h at RT and protein bands were revealed with chemiluminescence. Band intensities were quantified using ImageJ software.<sup>62</sup>

LC3-I was migrating as a double band in some experiments with the Sigma antibody used in this study. To understand whether one of the bands was a nonspecific band, we migrated cell extracts in parallel, blotted and incubated them with two different polyclonal LC3 antibodies, namely MBL antibody (PM036, raised against aa 1 to 120 of MAP1LC3B) and Sigma antibody (used in this study, L7543, raised against aa 2 to 15 of LC3B). Albeit the antibodies showed different affinities for LC3-I and LC3-II, both polyclonal antibodies revealed two LC3-I bands of similar sizes (Fig. S1). It is very unlikely that two different

polyclonal antibodies raised against two different polypeptides would reveal nonspecific bands of the same size. Therefore, we were convinced that both bands in LC3 blots corresponded to LC3-I forms and they were not nonspecific bands. Further studies are required to understand modification(s) leading to LC3-I double-band formation.

**RNA isolation and RT-PCR analysis.** Total RNA was extracted using TRIzol reagent (Sigma-Aldrich, T9424) according to the manufacturer's instructions. cDNA was reverse transcribed from total RNA (DNase treated) using M-MuLV reverse transcriptase (Fermentas, EP0351) and random hexamers (Invitrogen, 48190-011).

**Real-time RT-PCR for *ATG5* and *ATG12* mRNA quantification.** SYBR Green Quantitative RT-PCR kit (Roche, 04-913-914-001) and an iCycler iQ thermal cycler (BioRad) were used for single step qRT-PCR reactions. To activate the SYBR green, an initial cycle of 95°C, 10 min was performed followed by, PCR reactions: 40 cycles of 95°C for 15 sec and 60°C for 1 min. Then a thermal denaturation protocol was used to generate the dissociation curves for the verification of amplification specificity (a single cycle of 95°C for 60 sec, 55°C for 60 sec and 80 cycles of 55°C for 10 sec). Changes in mRNA levels were quantified using the  $2^{-\Delta\Delta CT}$  method using *GAPDH* (glyceraldehyde-3-phosphate dehydrogenase) mRNA as control. Primers used during the study were: *ATG5* primers 5'-TCA GCC ACT GCA GAG GTG TTT-3'; 5'-GGC TGC AGA TGG ACA GTT GCA-3'; *GAPDH* primers 5'-AGC CAC ATC GCT CAG ACA C-3'; 5'-GCC CAA TAC GAC CAA ATC C-3'; and *ATG12* primers 5'-CAG TTT ACC ATC ACT GCC AAA A-3'; 5'-ACA AAG AAG TGG GCA GTA GAG C-3'. Reactions were performed in duplicates and number of independent experiments (n) was marked.

**TaqMan RT-PCR for endogenous *MIR181A* quantification.** TaqMan qRT-PCR reactions were performed using FastStart Universal Probe Master kit (ROCHE, 04913957001) and an iCycler iQ thermal cycler (BioRad) according to the protocols described previously.<sup>23</sup> Primers and the probe used during the study were: Stem-loop primer, 5'-GTC GTA TCC AGT GCA GGG TCC GAG GTA TTC GCA CTG GAT ACG ACA ACT CAC CGA CAG CGT TGA ATG TT-3'. Forward primer, 5'-AAC ATT CAA CGC TGT CGG TGA GT-3'. Reverse primer, 5'-GTG CAG GGT CCG AGG T-3'. Probe, 5'(6-FAM)-CTG GAT ACG ACA ACT CAC-(TAMRA-sp)3'.

**Dual luciferase-reporter assay.** Vectors containing wild-type or mutated *MIR181A* MREs from *ATG5* 3' UTR were

cotransfected with *MIR181A* into 293T cells. Forty-eight hours later, cells were lysed. Firefly and renilla luciferase activities were measured using a dual luciferase-reporter assay system (Promega, E1910). Results were evaluated through normalization of the firefly luciferase activity with renilla luciferase activity.

**Antagomir tests.** miRIDIAN microRNA Hairpin Inhibitors (antagomirs) against hsa-mir181a (IH-30055307) and control antagomir miRIDIAN microRNA hairpin inhibitor negative control (IN001005-01-05) were purchased from Dharmacon. Negative control was based on cel-miR-67 (mature sequence: UCA CAA CCU CCU AGA AAG AGU AGA and Accession Number: MIMAT0000039), which has minimal sequence similarity with human miRNAs.

Transfection of antagomirs (200 nM) was performed using either the PEI transfection method<sup>23</sup> or AMAXA nucleofector (Lonza Nucleofector II AAD-1001S) with program E-014 and the Nucleofector kit V (Lonza, VCA-1003) according to the manufacturer's instructions.

**Statistical analyses.** Statistical analyses were performed using Student's two-tailed t-test. Data were represented as means of  $\pm$  SD of n independent experiments. Values of  $p < 0.05$  were considered as significant.

#### Disclosure of Potential Conflicts of Interest

No potential conflicts of interest were disclosed.

#### Acknowledgments

pCI-hApg5 and GFP-LC3 plasmids were kindly provided by Noboru Mizushima and Tomatsu Yoshimori, respectively. We would also like to thank Carlos le Sage for technical assistance, and Gozuacik Lab members and Stuart James Lucas for fruitful discussions and critical reading of the manuscript. K562 cells were a kind gift of Ayhan Bilir. This work was supported by the Scientific and Technological Research Council of Turkey (TUBITAK) 1001 Grant and Sabanci University. D.G. is a recipient of EMBO Strategic Development and Installation Grant (EMBO-SDIG) and Turkish Academy of Sciences (TUBA) GEBIP Award. G.K. and K.A.T. are recipients of Yousef Jameel and TUBITAK-BIDEB Scholarships, respectively. The authors have no financial conflict of interests.

#### Supplemental Materials

Supplemental materials may be found here: [www.landesbioscience.com/journals/autophagy/article/23117](http://www.landesbioscience.com/journals/autophagy/article/23117)

#### References

- Mizushima N. Autophagy: process and function. *Genes Dev* 2007; 21:2861-73; PMID:18006683; <http://dx.doi.org/10.1101/gad.1599207>
- Ravikumar B, Sarkar S, Davies JE, Futter M, Garcia-Arencibia M, Green-Thompson ZW, et al. Regulation of mammalian autophagy in physiology and pathophysiology. *Physiol Rev* 2010; 90:1383-435; PMID:20959619; <http://dx.doi.org/10.1152/physrev.00030.2009>
- Gozuacik D, Kimchi A. Autophagy as a cell death and tumor suppressor mechanism. *Oncogene* 2004; 23:2891-906; PMID:15077152; <http://dx.doi.org/10.1038/sj.onc.1207521>
- Mizushima N, Levine B. Autophagy in mammalian development and differentiation. *Nat Cell Biol* 2010; 12:823-30; PMID:20811354; <http://dx.doi.org/10.1038/ncb0910-823>
- Rubinsztein DC, Mariño G, Kroemer G. Autophagy and aging. *Cell* 2011; 146:682-95; PMID:21884931; <http://dx.doi.org/10.1016/j.cell.2011.07.030>
- Martinez-Vicente M, Cuervo AM. Autophagy and neurodegeneration: when the cleaning crew goes on strike. *Lancet Neurol* 2007; 6:352-61; PMID:17362839; [http://dx.doi.org/10.1016/S1474-4422\(07\)70076-5](http://dx.doi.org/10.1016/S1474-4422(07)70076-5)
- Kimmelman AC. The dynamic nature of autophagy in cancer. *Genes Dev* 2011; 25:1999-2010; PMID:21979913; <http://dx.doi.org/10.1101/gad.17558811>
- Mehrpour M, Esclatine A, Beau I, Codogno P. Overview of macroautophagy regulation in mammalian cells. *Cell Res* 2010; 20:748-62; PMID:20548331; <http://dx.doi.org/10.1038/cr.2010.82>
- Mizushima N, Yoshimori T, Ohsumi Y. The role of Atg proteins in autophagosome formation. *Annu Rev Cell Dev Biol* 2011; 27:107-32; PMID:21801009; <http://dx.doi.org/10.1146/annurev-cellbio-092910-154005>
- Kirisako T, Ichimura Y, Okada H, Kabeya Y, Mizushima N, Yoshimori T, et al. The reversible modification regulates the membrane-binding state of Apg8/Aut7 essential for autophagy and the cytoplasm to vacuole targeting pathway. *J Cell Biol* 2000; 151:263-76; PMID:11038174; <http://dx.doi.org/10.1083/jcb.151.2.263>



- 
59. Zhu W, Shan X, Wang T, Shu Y, Liu P. miR-181b modulates multidrug resistance by targeting BCL2 in human cancer cell lines. *Int J Cancer* 2010; 127:2520-9; PMID:20162574; <http://dx.doi.org/10.1002/ijc.25260>
60. Voorhoeve PM, le Sage C, Schrier M, Gillis AJ, Stoop H, Nagel R, et al. A genetic screen implicates miRNA-372 and miRNA-373 as oncogenes in testicular germ cell tumors. *Cell* 2006; 124:1169-81; PMID:16564011; <http://dx.doi.org/10.1016/j.cell.2006.02.037>
61. Oral O, Oz-Arslan D, Itah Z, Naghavi A, Deveci R, Karacali S, et al. Cleavage of Atg3 protein by caspase-8 regulates autophagy during receptor-activated cell death. *Apoptosis* 2012; 17:810-20; PMID:22644571; <http://dx.doi.org/10.1007/s10495-012-0735-0>
62. Abramoff MD, Magalhães PJ, Ram SJ. Image Processing with ImageJ. *Biophotonics International* 2004; 11:36-42